Structural characterization in solution of multifunctional nucleotide coordination systems

Juan A. Aguilar,[a] Bernardo Celda,[b] Vieri Fusi,[c] Enrique García-España,[d] Santiago V. Luis,[e] M[a] Carmen Martínez,[b] José A. Ramírez,[d] Conxa Soriano[a] and Roberto Tejero[b]

[a] *Departamento de Química Orgánica, Facultad de Farmacia, Universidad de Valencia, 46100 Burjassot (Valencia), Spain*
[b] *Departamento de Química Física, Facultad de Química, Universidad de Valencia, C/ Dr. Moliner 50, 46100 Burjassot (Valencia), Spain*
[c] *Instituto de Scienze Chimiche, Università di Urbino, P.zza Rinascimento 6, I-61209 Urbino, Italy*
[d] *Departamento de Química Inorgánica, Facultad de Química, Universidad de Valencia, C/ Dr. Moliner 50, 46100 Burjassot (Valencia), Spain*
[e] *Departamento de Química Orgánica e Inorgánica, Universidad Jaume I (Castellón) Spain*

Received (in Cambridge, UK) 7th January 2000, Accepted 31st March 2000
Published on the Web 2nd June 2000

The interaction in aqueous solution of the cyclophane receptors 2,6,10,13,17,21-hexaaza[22]orthocyclophane (**L**[1]) and 2,6,10,13,17,21-hexaaza[22]paracyclophane (**L**[2]) with the nucleotides ATP, ADP and AMP has been studied by pH titration and NMR. The obtained results are compared with those previously reported for the analogous *meta*-substituted receptor 2,6,10,13,17,21-hexaaza[22]metacyclophane (**L**). All the experimental data support the actuation of these cyclophane molecules as multi-point binders of nucleotides through electrostatic, hydrogen bonding and π-stacking interactions. The combined use of NMR and molecular dynamics permits us to get a rather reliable picture of the way in which the molecules organise in solution and how the intermolecular interactions (electrostatics, hydrogen bonding, π-stacking) are established.

Introduction

Anion co-ordination was recognised as a new field of chemistry in the late 1970's following the pioneering work of Lehn on this topic.[1] From then on, a great deal of experimental effort has been devoted to understanding and interpreting the role played by the different intermolecular forces controlling and regulating the association and recognition events in anion co-ordination chemistry. Among them, π-stacking between electron rich and electron poor aromatic clouds gains special importance in systems like these, since several weak intermolecular forces may effectively co-operate to achieve strong, but very often highly dynamic, overall interactions between host and guest species.[2]

Several multifunctional receptors incorporating condensed aromatic rings have been prepared in order to achieve co-ordination of nucleotide type anions through electrostatic, hydrogen bonding and π-stacking interactions.[3,4] We have also been exploring this topic and a couple of years ago we reported on the synthesis and anion coordination capabilities of the metacyclophane 2,6,10,13,17,21-hexaaza[22]metacyclophane (**L**).[5] This compound was one of the first examples of a receptor capable of interacting with nucleotides through electrostatic interactions between the phosphate chain of the nucleotide and the polyammonium sites of the macrocycle, and through π-stacking interactions between the adenosine residues and the phenylene subunit incorporated as a non-pendant integral part of the macrocyclic framework. Multinuclear NMR provided clear evidence for this.

Continuing with this research, here we communicate on the novel cyclophanes 2,6,10,13,17,21-hexaaza[22]orthocyclophane (**L**[1]) and 2,6,10,13,17,21-hexaaza[22]paracyclophane (**L**[2]), which are formally derived from **L** by changing the substitution of the aromatic ring, and we also show that these receptors recognize ATP, ADP and AMP in aqueous solution with participation of stacking interactions. Moreover, we provide a detailed structural NMR study and molecular dynamic analysis of the interaction of **L** with ADP in solution. The NMR study performed gives important information about the conformations of host and guest species and their intermolecular contacts.

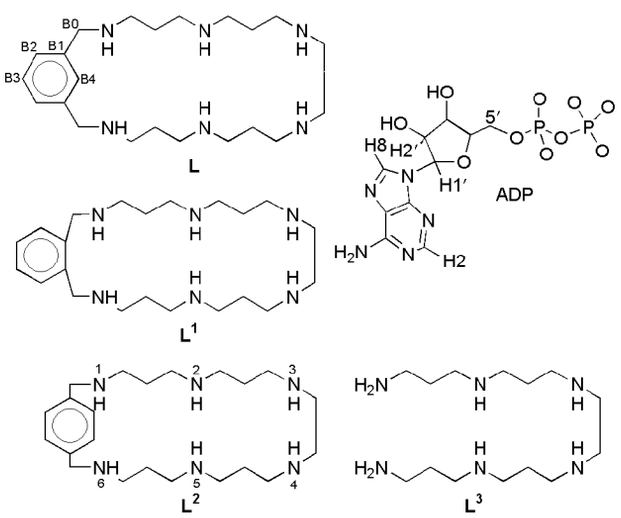

Chart 1

Experimental

Synthesis of the receptors

L[1] and **L**[2] were prepared as hexahydrochloride or hexaperchlorate salts following the general procedure described for **L** in

ref. 5 by reacting either 1,2-bis(bromomethyl)benzene or 1,3-bis(bromomethyl)benzene with *N*,*N*′,*N*″,*N*‴,*N*⁗,*N*⁗′-hexakis-(*p*-tolylsulfonyl)-1,5,9,12,16,20-hexaazacosane to afford **L**[1] and **L**[2], respectively, in their tosylated forms.

N,*N*′,*N*″,*N*‴,*N*⁗,*N*⁗′-Hexakis(*p*-tolylsulfonyl)-2,6,10,13,17,21-hexaaza[22]orthocyclophane (**L**[1]·6Ts)

Yield 40%, mp 181–183 °C. δ_H ($CDCl_3$) 1.50–1.54 (m, 4H), 1.81–1.85 (m, 4H), 2.38 (s, 12H), 2.42 (s, 6H), 2.87–3.14 (m, 16H), 3.28 (s, 4H), 4.48 (s, 4H), 7.22–7.33 (m, 16H), 7.51 (d, 4H), 7.61–7.71 (m, 8H). δ_C($CDCl_3$) 21.5, 29.0, 29.5, 46.4, 47.4, 47.7, 47.0, 48.2, 50.3, 127.0, 127.2, 127.4, 128.0, 129.0, 129.7, 129.9, 134.4, 135.2, 143.3. *m*/*z* (FAB) 1315 ([M + H]$^+$).

2,6,10,13,17,21-Hexaaza[22]orthocyclophane hexaperchlorate (**L**[1]·6$HClO_4$)

Liquid NH_3 (250 cm^3) was condensed into a suspension of **L**[1]·6Ts (3.95 g, 0.003 mol) in diethyl ether (30 cm^3) and methanol (1 cm^3) at −70 °C. Lithium was added in small portions (*ca.* 10 mg each); the stirred reaction mixture turned blue and then more lithium was added until the blue colour in the solution remained for at least 5 min. NH_4Cl (12 g, 0.02 mol) was then added in small amounts and the suspension warmed to room temperature. After evaporating all the NH_3 a white solid appeared which was treated with 3 mol dm^{-3} HCl and the obtained suspension washed three times with $CHCl_3$ (100 cm^3). The aqueous solution was filtered and the solvent vacuum evaporated to obtain a white solid that was then dissolved in a minimum amount of water and the resulting solution basified with concentrated NaOH. The solution was extracted with $CHCl_3$ (6 × 100 cm^3), the organic layer dried over Na_2SO_4 and vacuum evaporated to give 0.70 g of **L** as a colourless oil (yield 60%). The hexahydrochloride salt of **L**[1] was obtained quantitatively by cautiously adding excess of $HClO_4$ to an ethanolic solution of the free amine. (**CAUTION**: addition of $HClO_4$ to organic solutions can be dangerous and has to be conducted with care.) The white solid obtained was recrystallised from a water–ethanol solution (yield 75%). δ_H (D_2O) 2.08–2.12 (m, 8H), 3.12–3.28 (m, 16H), 3.43 (s, 4H), 4.31 (s, 4H), 7.45 (s, 4H). δ_C (D_2O) 21.9, 22.2, 42.1, 43.9, 44.1, 44.4, 45.1, 47.8, 130.2, 130.8, 130.9. Anal. Calcd for $C_{22}H_{48}N_6Cl_6O_{24}$: C, 26.6; H, 4.9; N, 8.5. Found: C, 26.5; H, 5.0; N, 8.4%.

N,*N*′,*N*″,*N*‴,*N*⁗,*N*⁗′-Hexakis(*p*-tolylsulfonyl)-2,6,10,13,17,21-hexaaza[22]paracyclophane (**L**[2]·6Ts)

Yield 34%, mp 268–270 °C. δ_H ($CDCl_3$) 1.60–1.67 (m, 4H), 1.78–1.83 (m, 4H), 2.36 (s, 6H), 2.38 (s, 6H), 2.41 (s, 6H), 2.97 (t, 4H), 3.07 (t, 4H), 3.12 (t, 4H), 3.28 (s, 4H), 3.93 (t, 4H), 4.23 (s, 4H), 7.20–7.26 (m, 12H), 7.32 (d, 4H), 7.54 (d, 4H), 7.68 (d, 4H), 7.70 (d, 4H). δ_C($CDCl_3$) 21.5, 28.9, 29.2, 46.9, 47.3, 48.0, 48.6, 52.9, 127.0, 127.1, 127.4, 128.9, 129.7, 129.8, 135.5, 135.8, 136.4, 143.2, 143.4, 143.5. *m*/*z* (FAB) 1315 ([M + H]$^+$).

2,6,10,13,17,21-Hexaaza[22]paracyclophane hexaperchlorate dihydrate (**L**[2]·6$HClO_4$·2H_2O)

The procedure was analogous to that described above for **L**[1] (yield 75%). δ_H (D_2O) 1.98–2.08 (m, 8H), 2.96–3.08 (m, 16H), 3.32 (s, 4H), 4.19 (s, 4H), 7.44 (s, 4H). δ_C (D_2O) 21.5, 22.9, 42.3, 43.3, 43.9, 44.5, 46.1, 50.9, 131.3, 131.6. Anal. Calcd for $C_{22}H_{52}N_6Cl_6O_{26}$: C, 25.7; H, 5.1; N, 8.2. Found: C, 25.8; H, 5.0; N, 8.0%.

Materials

The sodium salts of ATP, ADP and AMP were obtained from Boehringer-Mannheim. $NaClO_4$ used as supporting electrolyte was purified according to a published procedure.[6] All other chemicals were Merck reagent grade and were used without further purification. **L**[3] was obtained as its hexahydrobromide salt as described in ref. 7.

Emf Measurements

The potentiometric titrations were carried out at 298.1 ± 0.1 K in $NaClO_4$ (0.15 mol dm^{-3}). The experimental procedure used (burette, potentiometer, cell, stirrer, microcomputer, *etc.*) has been fully described elsewhere.[8] The acquisition of the emf data was performed with the computer program PASAT.[9] The reference electrode was an Ag/AgCl electrode in saturated KCl solution. The glass electrode was calibrated as an hydrogen-ion concentration probe by titration of previously standardised amounts of HCl with CO_2-free NaOH solutions and by determining the equivalence point by Gran's method,[10] which gives the standard potential, $E°$, and the ionic product of water (pK_w = 13.73(1)).

The computer program HYPERQUAD[11] was used to calculate the protonation and stability constants. The pH range investigated was 2.5–10.5 and the concentration of the different anions and of **L** ranged from 1×10^{-3} to 5×10^{-3} mol dm^{-3}. The protonation constants of **L** were taken from ref. 5 and the protonation constants of ATP, ADP and AMP from ref. 12.

The different titration curves for each system (*ca.* 100 experimental points corresponding to at least three measurements) were treated either as a single set or as separate curves without significant variations in the values of the stability constants. Finally, the sets of data were merged together and treated simultaneously to give the final stability constants. Moreover, several measurements were made both in formation and in dissociation (from acid to alkaline pH and *vice versa*) to check the reversibility of the reactions.

NMR Measurements

The ^{1}H and ^{13}C NMR spectra were recorded on Varian UNITY 300 and UNITY 400 spectrometers, operating at 299.95 and 399.95 MHz for ^{1}H and at 75.43 and 100.58 MHz for ^{13}C. The spectra were obtained at room temperature in D_2O or $CDCl_3$ solutions. For the ^{13}C NMR spectra, dioxane was used as a reference standard (δ = 67.4 ppm) and for the ^{1}H spectra, the solvent signal. The ^{31}P NMR spectra were recorded at 121.42 MHz on a Varian Unity 300 MHz. Chemical shifts are relative to an external reference of 85% H_3PO_4. A variable temperature accessory regulated the probe temperature. Adjustments to the desired pH were made using drops of HCl or NaOH solutions. The pH was calculated from the measured pD values using the correlation, pH = pD − 0.4.[13] For establishing the constraints in the molecular dynamic studies, total correlation spectroscopy (TOCSY) were recorded at three different mixing times (30, 50 and 70 ms) for the complete spin system identification.[14] NOE connectivities were obtained through rotating frame spectroscopy (ROESY)[15] at three different mixing times, 100, 150 and 600 ms (pH = 7, T = 298 K).

Molecular dynamics

The theoretical calculations were run on a Cray-Silicon Graphics Origin 2000 computer using the CHARMm MSI version as the forcefield.[16] Taking into account the NMR data, the distances were constrained between 2 and 6 Å. Calculations were performed in a 30 Å solvation sphere of TIP3 water molecules. The adduct (H_6LA^{3+}, A = ADP^{3-}) was then stacked into this solvation sphere and the water molecules at a distance closer than 2.6 Å from the macrocyclic cation were removed. The total number of water molecules surrounding the adduct species was 413.

The system was heated from 0 to 300 K for 20 ps and then equilibrated for the same time. Starting from the final structures of this equilibration four sets of 1 ns dynamic simulations were performed to complete 4 ns of molecular dynamics.

In the energy calculations, a 15 Å cut-off distance was employed with a switching function between 10 and 14 Å for the van der Waals terms. A set of 100 structures from the dynamics global coordinate file (each 40 ps) was selected and then minimised with 500 ABNR steps. For both dynamics and minimisation, the NMR constraints were applied.

Results and discussion

Basicity of the receptors

The stepwise protonation constants of the receptors **L**[1] and **L**[2] are shown in Table 1. The constants for the protonation steps of both receptors are similar until the fourth protonation. From then on, the constants of the *para*-substituted receptor are larger than those of the *ortho*-derivative. This is particularly remarkable for the fifth protonation step, for which a logarithmic difference of 1.5 is found ($\Delta\log K_{H_5L} = \log K_{H_5L^2} - \log K_{H_5L^1} = 1.5$). Interestingly enough, the basicity of the *para*-derivative (log $\beta = 50.62$, log $\beta = \Sigma$ log K_{H_iL}) is much closer to that of the *meta*-derivative (log $\beta = 50.33$)[5] than to that of the *ortho*-cyclophane (log $\beta = 48.16$). Also, the basicities of the *meta*- and *para*-cyclophanes (**L** and **L**[2]) are more similar to that of the open-chain polyamine **L**[3] (log $\beta = 51.01$) (see ligand drawing)[5,7] than to the basicity of the *ortho*-substituted cyclophane. Therefore, it seems that *ortho*-substitution has significant consequences for the conformation of the receptor and for the way in which the positive charges are distributed along the polyamine chain. All these characteristics are reflected in the distribution diagrams of **L**[1] and **L**[2] shown in Fig. 1.

Table 1 Logarithms of the stepwise protonation constants of receptors **L**[1] and **L**[2] determined in 0.15 mol dm^{-3} $NaClO_4$ at 298.1 K

Reaction[a]	**L**[1]	**L**[2]
$H + L \rightleftharpoons HL$	10.41(2)[b]	10.46(3)
$H + HL \rightleftharpoons H_2L$	9.85(2)	10.07(2)
$H + H_2L \rightleftharpoons H_3L$	8.98(3)	8.93(3)
$H + H_3L \rightleftharpoons H_4L$	7.69(3)	7.97(3)
$H + H_4L \rightleftharpoons H_5L$	5.94(3)	7.46(3)
$H + H_5L \rightleftharpoons H_6L$	5.29(3)	5.73(4)

[a] Charges omitted for clarity. [b] Values in parentheses are standard deviations in the last significant figure.

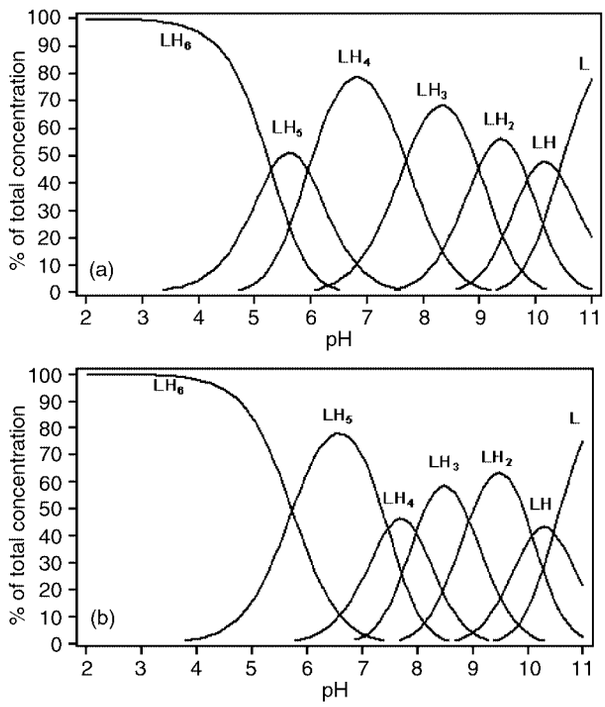

Fig. 1 Distribution diagrams for the systems H^+–**L**[1] (a) and H^+–**L**[2] (b).

Interaction with nucleotides: stability constants and selectivity trends

pH titrations show that both receptors **L**[1] and **L**[2] strongly interact with the nucleotides ATP, ADP and AMP (Table 2). The nucleotide : receptor stoichiometry of the adducts detected is always 1 : 1 and the extent of protonation varies from 1 to 8, in the pH range under study (3–10). The values for the stepwise formation constants of the adducts show that ATP is the substrate interacting most strongly with both receptors. In the ATP-systems and also in the ADP ones, the most important species in solution are H_6LA (A = ATP^{4-}, ADP^{3-}). Such species prevail in a wide pH range centred around neutral pH (see Fig. 2 for the systems **L**[1]–ATP and **L**[2]–ATP).

Since **L**[1], **L**[2] and the nucleotides participate in several overlapped protonation equilibria, care has to be taken in order to decide which equilibria are representative of the formation of

Table 2 Logarithms of the stability constants for the formation of adduct species between **L**[1], **L**[2] and the nucleotides ATP, ADP and AMP in 0.15 mol dm^{-3} $NaClO_4$ at 298.1 K

	AMP		ADP		ATP	
Reaction	**L**[1]	**L**[2]	**L**[1]	**L**[2]	**L**[1]	**L**[2]
$9H + A + L = AH_9L$[a]						
$8H + A + L \rightleftharpoons AH_8L$					63.10(2)	65.47(3)
$7H + A + L \rightleftharpoons AH_7L$	57.09(3)[b]	59.46(9)	57.7(1)	59.84(4)	60.30(2)	61.99(3)
$6H + A + L \rightleftharpoons AH_6L$	52.38(2)	54.95(3)	53.81(4)	55.35(2)	56.25(1)	57.27(2)
$5H + A + L \rightleftharpoons AH_5L$	46.80(2)	48.70(3)	47.41(5)	48.43(4)	48.89(2)	49.64(3)
$4H + A + L \rightleftharpoons AH_4L$	40.30(2)	41.36(3)	40.45(6)	40.92(4)	41.45(1)	41.88(3)
$3H + A + L \rightleftharpoons AH_3L$	32.58(2)	33.18(3)	32.87(6)	32.67(6)	32.90(2)	33.36(2)
$2H + A + L \rightleftharpoons AH_2L$	23.37(3)	24.09(5)	23.95(6)	23.56(7)	23.66(2)	24.00(3)
$H + A + L \rightleftharpoons AHL$	13.29(5)		14.43(6)	13.4(1)		
$H_2A + H_6L \rightleftharpoons H_8LA$					4.7	4.6
$HA + H_6L \rightleftharpoons H_7LA$	2.9	2.8	3.4	3.2	5.9	5.1
$HA + H_5L \rightleftharpoons H_6LA$	3.4	4.0	4.8	4.2	7.2	6.1
$A + H_6L \rightleftharpoons H_6LA$	4.2	4.3	5.7	4.7	8.1	6.7
$A + H_5L \rightleftharpoons H_5LA$	3.9	3.8	4.5	3.5	6.0	4.8
$A + H_4L \rightleftharpoons H_4LA$	3.4	3.9	3.5	3.5	4.5	4.5
$A + H_3L \rightleftharpoons H_3LA$	3.3	3.7	3.6	3.2	3.7	3.9
$A + H_2L \rightleftharpoons H_2LA$	3.1	3.6	3.7	3.0	3.4	3.5
$A + HL \rightleftharpoons HLA$	2.9		4.0	2.9		

[a] Charges omitted for clarity. [b] Values in parentheses are standard deviations in the last significant figure.

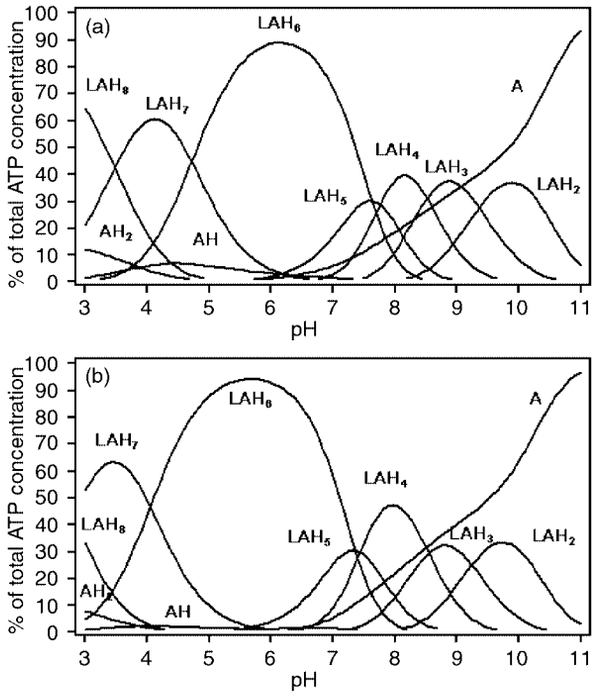

Fig. 2 Distribution diagrams for the systems ATP–$\mathbf{L}^1$ (a) and ATP–$\mathbf{L}^2$ (b). Concentration of all reagents 1×10^{-3} mol dm^{-3}.

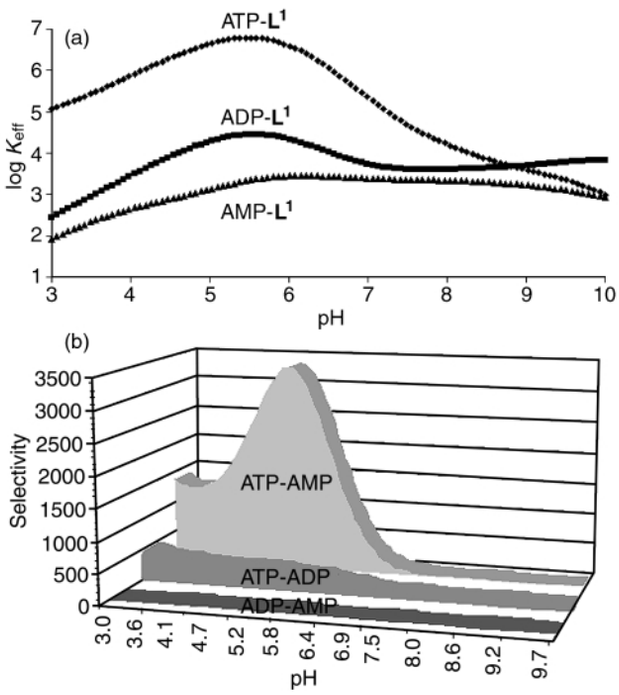

Fig. 3 (a) Plots of the conditional stability constant *vs.* pH for ATP–$\mathbf{L}^1$, ADP–$\mathbf{L}^1$ and AMP–$\mathbf{L}^1$. (b) pH Selectivity profile for the interaction of $\mathbf{L}^1$ with ATP, ADP and AMP. Concentration of all reagents 1×10^{-3} mol dm^{-3}.

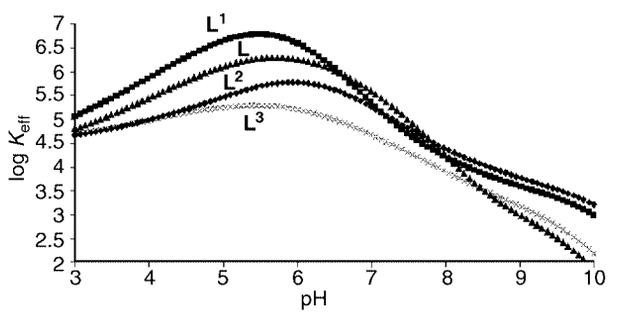

Fig. 4 Plots of the conditional stability constant *vs.* pH for the systems ATP–**L**, ATP–$\mathbf{L}^1$, ATP–$\mathbf{L}^2$ and ATP–$\mathbf{L}^3$. Concentration of all reagents 1×10^{-3} mol dm^{-3}.

the adduct species and, therefore, the real magnitude of the interaction between host and guest species. To overcome these difficulties several years ago some of us proposed a method based on calculating the distribution diagrams for the ternary system substrate A–substrate B–receptor, and representing the overall percentages of free and complexed substrates as a function of pH.[17] This method had the advantage of not requiring any assumption on the location of the protons in the host and guest species and allowed us to establish proper selectivity ratios.

More recently, we proposed a simpler definition of selectivity ratios based on the use of the classical conditional effective stability constants.[18] These calculations provide valuable clues for establishing the right protonation degrees of the intervening species.

For a given pH value, if the total amounts of free substrate ($\Sigma[H_iA]$), free receptor ($\Sigma[H_jL]$) and adduct formed ($\Sigma[H_{i+j}AL]$) are known one can define a conditional stability constant [eqn. (1)].

$$K_{\text{eff}} = \Sigma[H_{i+j}AL]/(\Sigma[H_iA] \times \Sigma[H_jL]) \qquad (1)$$

Fig. 3a shows plots of the logarithms of the conditional stability constants as a function of pH for the systems ATP–$\mathbf{L}^1$, ADP–$\mathbf{L}^1$ and AMP–$\mathbf{L}^1$. It can be seen that for ATP, the stability constants are clearly higher than those of the ADP and AMP adducts over a wide pH range. The quotients of the effective constants at a given pH allowed us to establish selectivity ratios and, for instance, at pH 5 the selectivity ratios ATP : ADP and ATP : AMP are *ca.* 230 and 3000, respectively. Fig. 3b shows a plot of the selectivity profile; the maximum selectivity ratios are reached for pH values around 6, where the hexaprotonated adduct predominates (see Fig. 2). This method allows comparison between any systems provided that the measurements have been carried out under the same experimental conditions. In the same way, Fig. 4 shows the conditional stability constants for the systems ATP–**L**, ATP–$\mathbf{L}^1$, ATP–$\mathbf{L}^2$ and ATP–$\mathbf{L}^3$ (see Chart 1). As can be seen, the values of stability constants in a wide pH range follow the order $\mathbf{L}^1 > \mathbf{L} > \mathbf{L}^2 > \mathbf{L}^3$. The open-chain polyamine would be the receptor interacting least with ATP, while the *ortho*-substituted cyclophane would be, among the cyclic receptors, the one displaying the larger stability constants. Therefore, it seems that *ortho*-substitution provides a conformation that favours interaction with anionic species such as nucleotides.

The analysis of the distribution diagrams for the binary and ternary systems and the values of the effective stability constants have allowed us to select the equilibria presented at the bottom of Table 2 as the correct ones for describing the formation of all adducts. It can be seen that in several cases two equilibria are required for defining the formation of the adducts. For instance, for the formation of $H_6(\mathbf{L}^1)A^{2+}$ (A = ATP^{4-}), equilibria (2) and (3) have to be considered.

$$HA^{3-} + H_5(\mathbf{L}^1)^{5+} \rightleftharpoons H_6(\mathbf{L}^1)A^{2+}, \log K = 7.2 \qquad (2)$$

or

$$A^{4-} + H_6(\mathbf{L}^1)^{6+} \rightleftharpoons H_6(\mathbf{L}^1)A^{2+}, \log K = 8.1 \qquad (3)$$

Obviously the extent of participation of each one will be changing throughout the pH range in which the adducts exist in solution.

Molecular dynamics studies

The 1D ^{1}H NMR spectrum (not shown) of the 1 : 1 mixture of ADP with **L** at pH 7.0 shows at least two pieces of evidence for

Table 3 Inter- and intramolecular NOEs for the ADP–**L** complex from the 400 MHz ROESY spectrum (τ_m = 150 ms) in D_2O at pH = 7.0[a] and 298 K

Proton	δ(ppm)	Proton	δ(ppm)	Upper limit/Å
H8	8.10	B4	7.20	6
H8	8.10	B2	7.03	6
H8	8.10	B0	3.86, 3.76	6
H2	7.83	B4	7.20	6
H2	7.83	B2	7.03	6
H2	7.83	B0	3.86, 5.76	6
H1′	5.74	B4	7.20	6
H4′	4.18	B4	7.20	6
H5′	4.01	B4	7.20	6
H5′	4.01	B0	3.86, 3.76	6
H8	8.10	H1′	5.74	5
H8	8.10	H2′	4.58	4
H8	8.10	H3′	4.33	5
H8	8.10	H4′	4.18	5
H8	8.10	H5′	4.01	6
H1′	5.74	H2′	4.58	5
H1′	5.74	H3′	4.33	5
H1′	5.74	H4′	4.18	5
H1′	5.74	H5′	4.01	6

[a] Without correction.

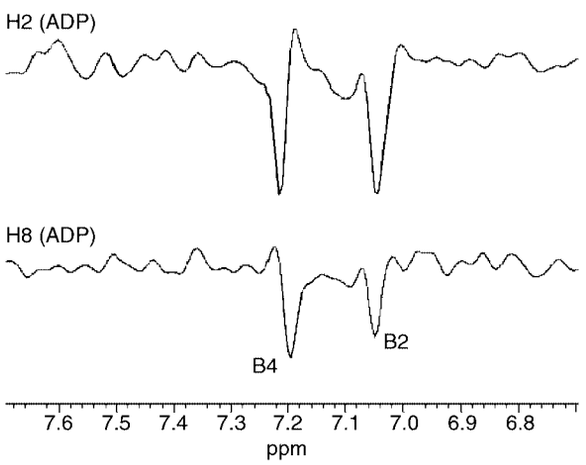

Fig. 5 Cross-sections along w_2 at w_1 = 8.10 ppm (ADP H8 proton) and w_1 = 7.83 ppm (ADP H2 proton) in the ROESY spectrum of the ADP–**L** 1 : 1 complex in D_2O (--- M; pH = 7.0; 400 MHz; τ_m = 150 ms).

complexation. These are, first, the chemical shifts of a large number of host and guest signals compared to those of the free compounds and, second, the strong line broadening of the nucleotide.[19] Nevertheless, the most reliable evidence for the complex structure can be obtained from studies of the *intermolecular* NOE. As shown in Table 3 and in Fig. 5, there are NOE cross-peaks in a ROESY experiment (150 ms mixing time) between H8 and H2 protons of the adenine ring of ADP and B4 and B2 protons of the macrocyclic receptor **L**. This observation clearly indicates a spatial proximity between both aromatic rings, the phenylene subunit of **L** and the adenine moiety of ADP. Such interactions have been shown to provide semi-quantitative information about distances of the complex geometry[19,20] and for this reason the upper limit of NOE restraints has been fixed at 6 Å. The distances have been constrained between 2 and 6 Å for those protons for which *inter*- and *intramolecular* NOE have been observed (Table 3). Particularly interesting are the NOEs observed between B4 protons of the macrocyclic receptor **L** and protons H1′, H4′ and H5′ of the sugar moiety. The NOE detected between H5′ and B0(a) and B0(b) protons have also been useful for geometry calculations of the adduct. A total of 15 *intermolecular* NOE from ROESY experiments (Table 3) have been used as restraints for molecular dynamics simulations of the ADP–

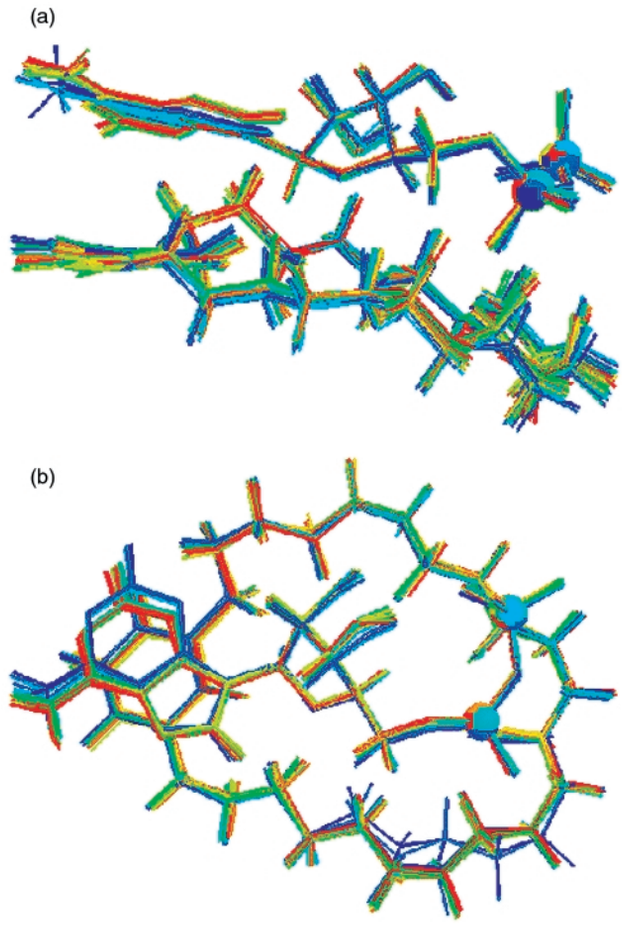

Fig. 6 Frontal (a) and top (b) views of a family of 28 lowest energy conformations of ADP–**L** 1 : 1 complex from a 4 ns RMD calculation in a solvation sphere of water (TIP3) of diameter 30 Å. Water molecules have been omitted, and phosphate atoms are shown in CPK form.

metacyclophane complex structure. In addition, 8 *intramolecular* NOEs have also been used as constraints for ADP structure determination in the adduct. The upfield chemical shift variations of B2, B3 and B4 protons of macrocyclic receptor **L** and H8 and H2 in ADP, and the NOEs observed between aromatic protons in both receptor **L** and ADP clearly indicate a close interaction between the aromatic rings. These experimental data were used as starting empirical information for initial docking between **L** and ADP. A long restrained molecular dynamics (RMD) simulation (4 ns) using the whole set of *inter*- and *intramolecular* NOEs and in a solvation sphere of water (TIP3) of 30 Å in diameter was then carried out. A structure of the **L**–ADP complex was extracted and the energy minimised every 40 ps, giving a set of 100 **L**–ADP complex conformations. The superposition of 27 structures with an energy difference lower than 25 kcal mol^{-1} is shown in Fig. 6. For this cluster of lower energy structures no NOE violations greater than 0.5 Å were observed. A π-stacking interaction between both aromatic rings can clearly be observed (Fig. 6), whereas the electrostatic interaction between the negative charges of ADP phosphates and the positive charges of the **L** macrocycle is preserved.

In general, bond distances (P–O) and angles (P–O–P, P–O–C and O–P–O) as well as torsion angles (pseudo-rotation angles) for calculated ADP conformations with the **L**–ADP complex are in good agreement with the literature.[21,22] The P–O distances for the calculated structures are between 1.58 and 1.62 Å.[22] The average P–O–P bond angle value reported in the literature is 130° whereas the average value for the calculated structures is 132.8°. A similar agreement is obtained for the P–O–C bond angle, *ca.* 120° for the reported values and 118.8° for the calcu-

lated structures. The O–P–O bond angle is a function of substituents on O, and the literature values are in the range 100–120° whereas the average experimental value is 111.6°. Due to the average values of O–P–O and P–O–P bond angles (100 and 130°, respectively) in the calculated ADP–**L** complex structures a large conformational freedom for the O–P–O–P dihedral angle can be expected.

The relative orientation between the sugar moiety and the phosphate fragment is close to the *anti* conformation in the more relaxed **L**–ADP complex structures, as can be deduced from the distances between the C8 and C2 carbons of the adenosine and the C5′, O5′ and P1 atoms. The *anti* conformation is the most favorable.[23,24] The preferred conformation for the C5′–O5′ bond in a large number of mononucleotides is (*gauche*)′–(*gauche*)′.[25] For the most stable calculated structures (Fig. 6) of the **L**–ADP complex the most populated conformation is (*gauche*)′–(*gauche*)′ almost eclipsed. The puckering of the ribose moiety, defined through the pseudorotation angle (*P*), is close to C3′ *endo* ($P = 29°$) ($^3T_4$ conformation), which is in agreement with the most stable conformation of the ribose and deoxyribose sugars, C3′ *endo* ($P = 0–36°$) and C2′ ($P = 144–180°$).

In all calculated structures of ADP–**L**, π-stacking can be clearly observed between the aromatic rings of ADP and **L** (see Fig. 6). The distance between the average planes of the adenine ring of the nucleotide and the benzene ring of the macrocycle is 3.38 Å and the mean angle between both planes is 4.229°. Likewise, the phosphate group lies parallel to macrocycle **L**. The electrostatic interactions seem to be more important between the phosphate groups of ADP and the nitrogen atoms opposed to the phenyl ring in **L**, particularly N3 and N4 and to a lesser extent N2. For the whole set of the **L**–ADP structures the distance between the phosphorus atoms and N3, N4 (and N2) is always <4 Å. It should be noted that hydrogen bonding is possible between the adenine nitrogen and/or the OH groups of the ribose subunits and the polyammonium benzylic groups of the receptor. This hydrogen bonding could reduce the mobility of that part of the molecule (Fig. 6) and partially stabilise the adduct, which would also explain the splitting of the benzylic signals of the receptor.[5] A hydrogen bond between the N3 of the adenine and the benzylic groups of the receptor has been observed in 64% of the structures calculated for the **L**–ADP complex. On the other hand, only in 4% of the calculated structures of the adducts has a direct hydrogen bond between N atoms of **L** and the phosphate groups of ADP been detected.

The experimental results, in particular NOE connectivities, for the **L**–ADP complex clearly show the direct participation of π-stacking interactions in molecular recognition in supramolecular systems.

Acknowledgements

We are indebted to DGICYT Project no. PB96-0796-CO2 and Generalitat Valenciana Project no. GV-D-CN-09-140 for financial support.

References

1 J.-M. Lehn, *Angew. Chem.*, *Int. Ed. Engl.*, 1988, **27**, 89; J.-M. Lehn, *Supramolecular Chemistry*, *Concepts and Perspectives*, VCH, 1995.
2 *Supramolecular Chemistry of Anions*, eds. A. Bianchi, K. Bowman-James and E. García-España, Wiley-VCH, New York, 1997.
3 J. Rebek, Jr., *Science*, 1987, **235**, 1478; A. D. Hamilton and D. J. Van Engen, *J. Am. Chem. Soc.*, 1987, **109**, 5035; M. W. Hosseini, J.-M. Lehn and M. P. Mertes, *Helv. Chim. Acta*, 1983, **66**, 2454; M. Shionaya, T. Ikeda, E. Kimura and S. Motoo, *J. Am. Chem. Soc.*, 1994, **116**, 3848; P. Cudic, M. Zinic, V. Tomisic, V. Simeon, J.-P. Vigneron and J.-M. Lehn, *J. Chem. Soc.*, *Chem. Commun.*, 1995, 1073; K. G. Ragunathan and H.-J. Schneider, *J. Chem. Soc.*, *Perkin Trans. 2*, 1996, 2597.
4 M. W. Hosseini, A. J. Blacker and J.-M. Lehn, *J. Am. Chem. Soc.*, 1990, **112**, 3896; H. Fenniri, M. W. Hosseini and J.-M. Lehn, *Helv. Chim. Acta*, 1997, **80**, 786.
5 J. A. Aguilar, E. García-España, J. A. Guerrero, S. V. Luis, J. M. Llinares, J. A. Ramírez and C. Soriano, *J. Chem. Soc.*, *Chem. Commun.*, 1995, 2237; J. A. Aguilar, E. García-España, J. A. Guerrero, S. V. Luis, J. M. Llinares, J. A. Ramírez and C. Soriano, *Inorg. Chim. Acta*, 1996, **246**, 287.
6 M. Micheloni, P. May and D. R. Williams, *J. Inorg. Nucl. Chem.*, 1978, **40**, 1209.
7 J. A. Aguilar, A. Bianchi, E. García-España, S. V. Luis, J. M. Llinares, J. A. Ramírez and C. Soriano, *J. Chem. Soc.*, *Dalton Trans.*, 1994, 637.
8 E. García-España, M.-J. Ballester, F. Lloret, J.-M. Moratal, J. Faus and A. Bianchi, *J. Chem. Soc.*, *Dalton Trans.*, 1988, 101.
9 M. Fontanelli and M. Micheloni, *Proceedings of the 1st Spanish–Italian Congress on Thermodynamics of Metal Complexes*, Diputación de Castellón, Castellón, Spain, 1990.
10 G. Gran, *Analyst*, 1952, **77**, 881; F. J. Rossotti and H. Rossotti, *J. Chem. Educ.*, 1965, **42**, 375.
11 A. Sabatini, A. Vacca, A. Gans and P. Gans, *Coord. Chem. Rev.*, 1992, **120**, 389.
12 Protonation constants of ATP, ADP and AMP were taken from A. Bencini, A. Bianchi, E. García-España, E. C. Scott, L. Morales, B. Wang, T. Deffo, F. Takusagawa, M. P. Mertes, K. Bowman Mertes and P. Paoletti, *Bioorg. Chem.*, 1992, **20**, 8.
13 A. K. Convington, M. Paabo, R. A. Robinson and R. G. Bates, *Anal. Chem.*, 1968, **40**, 700.
14 L. Braunschweiler and R. R. Ernst, *J. Magn. Reson.*, 1983, **53**, 521.
15 A. A. Bother-By, R. L. Stephens, J. M. Lee, C. D. Warren and R. W. Jeanloz, *J. Am. Chem. Soc.*, 1984, **106**, 811.
16 CHARMm, Molecular Simulations Inc, 16 New England Executive Park, Burlington, MA, 01803-5297 USA.
17 A. Andrés, J. Aragó, A. Bencini, A. Bianchi, A. Doménech, V. Fusi, E. García-España, P. Paoletti and J. A. Ramírez, *Inorg. Chem.*, 1993, **32**, 3418; A. Bencini, A. Bianchi, M. I. Burguete, P. Dapporto, A. Doménech, E. García-España, S. V. Luis, P. Paoli and J. A. Ramírez, *J. Chem. Soc.*, *Perkin Trans. 2*, 1994, 569.
18 M. T. Albelda, M. A. Bernardo, E. García-España, M. L. Godino Salido, S. V. Luis, M. J. Melo, F. Pina and C. Soriano, *J. Chem. Soc.*, *Perkin Trans. 2*, 1999, 2545.
19 A. V. Eliseev and H.-J. Schneider, *J. Am. Chem. Soc.*, 1994, **116**, 6081.
20 C. A. Hunter, *Chem. Soc. Rev.*, 1994, **23**, 101.
21 W. Saenger, *Principles of nucleic acid structure*, Springer-Verlag, USA, 1984.
22 B. S. Reddy, W. Saenger, K. Mühlegger and G. Weimann, *J. Am. Chem. Soc.*, 1981, **103**, 907.
23 S. I. Chan and J. H. Nelson, *J. Am. Chem. Soc.*, 1969, **91**, 168.
24 H. P. Schweizer, A. D. Brown, P. O. P. Ts'o and D. P. Hollis, *J. Am. Chem. Soc.*, 1968, **90**, 1042.
25 R. H. Sarma, R. J. Mynott, D. J. Wood and F. E. Hruska, *J. Chem. Soc.*, *Chem. Commun.*, 1973, 140.